A New Model of Trapping and Relative Permeability Hysteresis for All Wettability Characteristics

Elizabeth J. Spiteri, SPE, Chevron Energy Technology Company; **Ruben Juanes,** SPE, Massachusetts Institute of Technology; **Martin J. Blunt,** SPE, Imperial College London; and **Franklin M. Orr, Jr.,** SPE, Stanford University

Summary

The complex physics of multiphase flow in porous media are usually modeled at the field scale using Darcy-type formulations. The key descriptors of such models are the relative permeabilities to each of the flowing phases. It is well known that, whenever the fluid saturations undergo a cyclic process, relative permeabilities display hysteresis effects.

In this paper, we investigate hysteresis in the relative permeability of the hydrocarbon phase in a two-phase system. We propose a new model of trapping and waterflood relative permeability, which is applicable for the entire range of rock wettability conditions. The proposed formulation overcomes some of the limitations of existing trapping and relative permeability models. The new model is validated by means of pore-network simulation of primary drainage and waterflooding. We study the dependence of trapped (residual) hydrocarbon saturation and waterflood relative permeability on several fluid/rock properties, most notably the wettability and the initial water saturation. The new model is able to capture two key features of the observed behavior: (1) nonmonotonicity of the initial-residual curves, which implies that waterflood relative permeabilities cross; and (2) convexity of the waterflood relative permeability curves for oil-wet media caused by layer flow of oil.

Introduction

Hysteresis refers to irreversibility or path dependence. In multiphase flow, it manifests itself through the dependence of relative permeabilities and capillary pressures on the saturation path and saturation history. From the point of view of pore-scale processes, hysteresis has at least two sources: contact angle hysteresis, and trapping of the nonwetting phase.

The first step in characterizing relative permeability hysteresis is the ability to capture the amount of oil that is trapped during any displacement sequence. Indeed, a trapping model is the crux of any hysteresis model: it determines the endpoint saturation of the hydrocarbon relative permeability curve during waterflooding.

Extensive experimental and theoretical work has focused on the mechanisms that control trapping during multiphase flow in porous media (Geffen et al. 1951; Lenormand et al. 1983; Chatzis et al. 1983). Of particular interest to us is the influence of wettability on the residual hydrocarbon saturation. Early experiments in uniformly wetted systems suggested that waterflood efficiency decreases with increasing oil-wet characteristics (Donaldson et al. 1969; Owens and Archer 1971). These experiments were performed on cores whose wettability was altered artificially, and the results need to be interpreted carefully for two reasons: (1) reservoirs do not have uniform wettability, and the fraction of oil-wet pores is a function of the topology of the porous medium and initial water saturation (Kovscek et al. 1993); and (2) the coreflood experiments were not performed for a long enough time, and not enough pore volumes were injected to drain the remaining oil layers to achieve ultimate residual oil saturation. In other coreflood experiments, in which many pore volumes were injected, the observed trapped/residual saturation did not follow a monotonic trend as a function of wettability, and was actually lowest for intermediate-wet to oil-wet rocks (Kennedy et al. 1955; Moore and Slobod 1956; Amott 1959). Jadhunandan and Morrow (1995) performed a comprehensive experimental study of the effects of wettability on waterflood recovery, showing that maximum oil recovery was achieved at intermediate-wet conditions.

An empirical trapping model typically relates the trapped (residual) hydrocarbon saturation to the maximum hydrocarbon saturation; that is, the hydrocarbon saturation at flow reversal. In the context of waterflooding, a trapping model defines the ultimate residual oil saturation as a function of the initial water saturation. The most widely used trapping model is that of Land (1968). It is a single-parameter model, and constitutes the basis for a number of relative permeability hysteresis models. Other trapping models are those of Jerauld (1997a) and Carlson (1981). These models are suitable for their specific applications but, as we show in this paper, they have limited applicability to intermediate-wet and oil-wet media.

Land (1968) pioneered the definition of a "flowing saturation," and proposed to estimate the imbibition relative permeability at a given *actual* saturation as the drainage relative permeability evaluated at a modeled *flowing* saturation. Land's imbibition model (1968) gives accurate predictions for water-wet media (Land 1971), but fails to capture essential trends when the porous medium is weakly or strongly wetting to oil. The two-phase hysteresis models that are typically used in reservoir simulators are those by Carlson (1981) and Killough (1976). A three-phase hysteresis model that accounts for essential physics during cyclic flooding was proposed by Larsen and Skauge (1998). These models have been evaluated in terms of their ability to reproduce experimental data (Element et al. 2003; Spiteri and Juanes 2006), and their impact in reservoir simulation of water-alternating-gas injection (Spiteri and Juanes 2006; Kossack 2000). Other models are those by Lenhard and Parker (1987), Jerauld (1997a), and Blunt (2000). More recently, hysteresis models have been proposed specifically for porous media of mixed wettability (Lenhard and Oostrom 1998; Moulu et al. 1999; Egermann et al. 2000).

All of the hysteresis models described require a bounding drainage curve and either a waterflood curve as input, or a calculated waterflood curve using Land's model. The task of experimentally determining the bounding waterflood curves from core samples is arduous, and the development of an empirical model that is applicable to non-water-wet media is desirable. In this paper, we introduce a relative permeability hysteresis model that does not require a bounding waterflood curve, and whose parameters may be correlated to rock properties such as wettability and pore structure.

Because it is difficult to probe the full range of relative permeability hysteresis for different wettabilities experimentally, we use a numerical tool—pore-scale modeling—to predict the trends in residual saturation and relative permeability. As we discuss later, pore-scale modeling is currently able to predict recoveries and relative permeabilities for media of different wettability reliably (Dixit et al. 1999; Øren and Bakke 2003; Jackson et al. 2003; Valvatne and Blunt 2004; Al-Futaisi and Patzek 2003, 2004). We

This paper (SPE 96448) was first presented at the 2005 SPE Annual Technical Conference and Exhibition, Dallas, 9–12 October, and revised for publication. Original manuscript received for review 21 July 2005. Revised manuscript received 11 April 2007. Paper peer approved 23 January 2008.

will use these predictions as a starting point to explore the behavior beyond the range probed experimentally.

In summary, this paper presents a new model of trapping and waterflood relative permeability, which is able to capture the behavior predicted by pore-network simulations for the entire range of wettability conditions.

Pore-Scale Modeling of Trapping and Hysteresis

In pore-network modeling, the pore space is described by a network of pores connected by throats with an idealized geometry. A set of physically based rules describe the configuration of the fluids within each pore and throat, as well as the mechanisms for the displacement of one fluid by another. This approach was pioneered by Fatt (1956) and has received increasing attention over the past decade. Blunt (2001) and Blunt et al. (2003) provide a detailed description of the fundamentals and applications of pore-network modeling, together with an extensive literature review. One of the successful application areas of pore-network models is the prediction of multiphase flow properties, such as capillary pressure and relative permeability. This success hinges on the following:

1. The ability to reproduce the essential geometric features of the pore space of real rocks. A realistic 3D pore-space characterization may be obtained in a variety of ways: assembly of 2D sections to form a 3D image (Holt et al. 1996); direct X-ray microtomography of the 3D pore space (Spanne et al. 1994); stochastic 3D modeling with statistics inferred from 2D thin sections (Ioannidis and Chatzis 2000); and process-based reconstruction in which grain deposition, compaction, and cementation are modeled (Bryant and Blunt 1992; Øren and Bakke 2002).

2. The ability to capture wettability effects. Most pore-network models used today introduce wettability effects based on the pore-level scenario of wetting proposed by Kovscek et al. (1993). Their model mimics the saturation change typical of a hydrocarbon reservoir. The medium is initially filled with water, and the rock surfaces are water-wet. During oil migration, the oil invades the pore space, altering the wettability of the solid surface in contact with the oil. In this fashion, the network displays mixed wettability: a fraction of a pore or throat may be oil-wet, while the corners and crevices not in contact with the oil remain water-wet.

The combination of realistic pore geometry/topology and correct characterization of displacement and trapping mechanisms has allowed pore-network models to predict hysteretic capillary pressure and relative permeability curves under a wide range of wettability characteristics.

Experimental measurements of hysteretic relative permeability for mixed-wet and oil-wet media are scarce (Jadhunandan and Morrow 1995; Oak 1991). Given the success of pore-network models to reproduce experimental data (Øren and Bakke 2003; Jackson et al. 2003; Valvatne and Blunt 2004), in this work we have adopted the use of pore-network modeling as a way to investigate the full spectrum of wettability conditions. Pore-network simulations results are taken as "data" to develop and validate empirical trapping and hysteresis models.

Description of the Pore-Network Simulations. We used the two-phase flow pore-network simulator developed by Valvatne and Blunt (2004). The model has similarities with other network models (Al-Futaisi and Patzek 2003; Øren et al. 1998; Patzek 2001). A full description of the model is given in the previous references.

We used a 3D pore-network of a Berea sandstone developed by Bakke and Øren (1997). The model is a cube of 3×3×3 mm^3 containing 12,349 pores and 26,146 throats. The absolute permeability of the rock is 2287 md and the net porosity is 0.183, where 0.0583 is clay-bound or microporosity.

We investigated sequences of two consecutive displacements: primary drainage (oil invasion) and waterflooding. During primary oil drainage the network, which is initially filled with water, is assumed to be strongly water-wet with a receding contact angle $\theta_r = 0°$. As the oil invades the largest pores first in piston-like displacement, the water recedes and is squeezed to the crevices and pore throats until a very high capillary pressure or a target oil saturation is reached. At this point, the surface of the rock in contact with oil will undergo wettability alteration, while the corners and elements that still contain only water remain strongly water-wet. Wettability alteration is accounted for by changing the contact angle. In principle, one could change the advancing contact angle θ_a and the receding contact angle θ_r independently. In this work, however, we used a correlation proposed by Morrow (1975) to link both the advancing and receding contact angles with an intrinsic contact angle θ_i. This relationship is shown in **Fig. 1.**

During waterflooding, there are several physical mechanisms by which the water can displace the oil in place (Lenormand et al. 1983). These mechanisms include piston-type displacement, cooperative pore-body filling, and snap-off. The predominance of any given displacement mechanism is strongly dependent on the wettability (specified by the advancing contact angle). These displacement processes and their implementation are described in detail in the literature (Valvatne and Blunt 2004; Al-Futaisi and Patzek 2003; Øren et al. 1998; Patzek 2001). After individual displacement events, the transport properties are calculated. The equations for absolute permeability, relative permeability, and other transport parameters can also be found in the literature (Valvatne and Blunt 2004; Øren et al. 1998; Patzek 2001; Blunt and King 1991). Following this procedure, pore-network simulations have been shown to reproduce experimental capillary pressure and relative permeability curves both in primary drainage and waterflooding (Øren et al. 1998) and for a variety of wettability conditions (Øren and Bakke 2003; Jackson et al. 2003; Valvatne and Blunt 2004).

We investigated the full range of wetting conditions after wettability alteration, by choosing average intrinsic contact angles between 20 and 160°. Because of pore-scale inhomogeneities in the rock minerals and surface roughness, assigning a uniform contact angle throughout is unrealistic. Therefore, we assigned contact angles throughout the network randomly within ±20° of the average value.

In this work, we assume that the contact angle distribution in originally oil-filled pores is independent of S_{oi}. In reality, a higher S_{oi} represents a larger initial capillary pressure that may cause protective water layers to collapse in oil-filled pores, causing a more significant wettability alteration than for low S_{oi} (Kovscek et al. 1993). However, this simple characterization of wettability has been shown to be sufficient to predict trends in recovery seen experimentally (Valvatne and Blunt 2004). Also, we consider systems in which there is a relatively uniform distribution of wettability—we do not consider mixed-wet media where initially oil-filled pores may be water-wet or oil-wet with two distinct distributions of contact angle in the same rock.

For each contact angle distribution we performed a series of displacement pairs (oil invasion and waterflooding), with a differ-

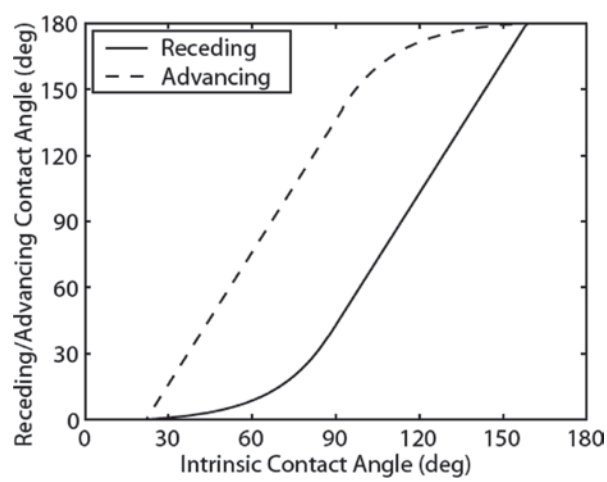

Fig. 1—Relationship between receding and advancing contact angles on a rough surface, as a function of intrinsic contact angle measured at rest on a smooth surface (Morrow 1975) (Fig. from Valvatne and Blunt 2004).

ent target oil saturation S_{oi} ranging from a very small value (almost no oil invasion) to the maximum value possible (connate water conditions). Next, we present results from an extensive set of simulations for different contact angles and different target oil saturations.

Pore-Network Predictions of Trapping. The use of a pore-network simulator allows us to quantify the effects of wettability and initial oil saturation on the trapping of oil during waterflooding. The main results of the pore-network simulations are compiled in **Fig. 2,** where we plot the initial-residual (IR) curves for different intrinsic contact angles. For a given curve (i.e., for a specific value of the intrinsic contact angle after wettability alteration), each point denotes the trapped oil saturation S_{ot} that corresponds to a particular initial oil saturation S_{oi}. The initial oil saturation is dictated by the point at which primary drainage ceases (and waterflood starts), and the trapped oil saturation is the value of unrecoverable (or residual) oil after waterflooding.

The most noteworthy characteristic of the IR curves shown in Fig. 2 is that they do not display a monotonically increasing behavior for mixed-wet and oil-wet media. This means that, for oil-wet media, higher oil saturation after the initial oil invasion may lead to lower residual oil saturation after waterflooding. This counterintuitive behavior is analyzed and explained next, in terms of pore-scale fluid configurations and displacement mechanisms.

For water-wet media (small contact angles), trapping during waterflooding is controlled by snap-off. As the initial oil saturation is increased, oil is pushed into smaller and smaller pores. During waterflooding, water fills the smallest pores first and snaps off more and more oil. The amount of trapped oil increases monotonically with increasing initial oil saturation simply because there is more oil to trap. As the contact angle increases, there is a crossover from trapping by snap-off to trapping by bypassing, as the water tends to advance in a connected front with piston-like advance on throats and cooperative pore-filling. We begin to see a non-monotonic behavior because, as the initial water saturation increases, we have more water filling from the pores and throats in connected patches from throats that are initially water-filled. When these patches join up, there can be trapping, as oil becomes stranded between these clusters. Low initial water saturation (i.e., high initial oil saturation) implies that there are few water clusters and little chance for bypassing. Trapping increases as the number of clusters increases and then declines again as there is less oil to trap in the first place. For intrinsic contact angles above 90° (advancing contact angles greater than 120°), we observe the same behavior, but with even less trapping. The reason is the presence of oil layers within the network. Water fills the largest pores and throats in an invasion percolation-like process. Oil remains connected in layers sandwiched between water in the center of an element and water in the corners. These layers lead to very little trapping, although the oil relative permeability is very low. These layers are stable until the two water/oil interfaces meet. High initial water saturation means that water bulges out in the corners causing these interfaces to meet, trapping more oil than for low initial water saturation. Again, for sufficiently large S_{wi}, (low S_{oi}), there is less trapping simply because there is less oil to trap.

We should also mention that the extremely low trapped oil saturations for very high initial oil saturations are an artifact of the criterion used for ascertaining the stability of oil layers (Valvatne and Blunt 2004). In the future, we plan to incorporate a stability criterion based on free-energy balance that predicts that oil layers become unstable before the two water/oil interfaces touch each other (van Dijke et al. 2004). For practical purposes, however, such high initial oil saturations are never achieved during migration of oil into realistic reservoirs—the initial water saturation is typically much higher than 5%.

In conclusion, the trapping mechanisms that we have indicated allow for a physical explanation of the non-monotonic behavior of the initial-residual curves. A complete picture of the trapping relation is given in **Fig. 3** as a trapping surface; that is, a surface that describes the residual oil saturation as a function of the initial oil saturation and the intrinsic contact angle after wettability alteration.

The trapped oil saturation dictates the endpoint of the relative permeability waterflood curves. An important practical consequence of the nonmonotonic relation of trapped vs. initial oil saturation for mixed- to oil-wet media is that waterflood scanning curves will cross, as sketched in **Fig. 4.**

Neither of these features—nonmonotonic trapping relation and crossover of waterflood relative permeability curves—are present in existing empirical models. This motivates the development of new empirical trapping and hysteresis models that reproduce the observed behavior.

Pore-Network Predictions of Waterflood Relative Permeability. It is important to understand the trapping mechanisms that ultimately define the shape of the relative permeability curves during waterflooding. The trapping model determines the endpoint residual saturations when the capillary pressure is lowered to an extremely low value. The trapping mechanisms at this point should

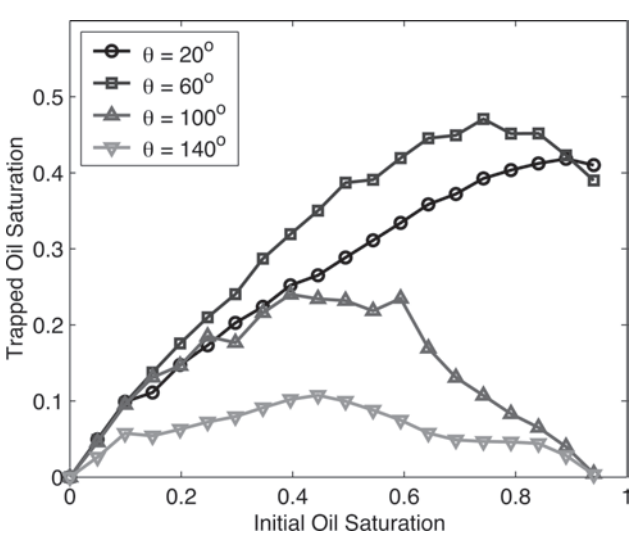

Fig. 2—Trapped oil saturation (S_{ot}) as a function of the initial oil saturation (S_{oi}) for different intrinsic contact angles (θ). Note that the curves are nonmonotonic except for strongly water-wet media.

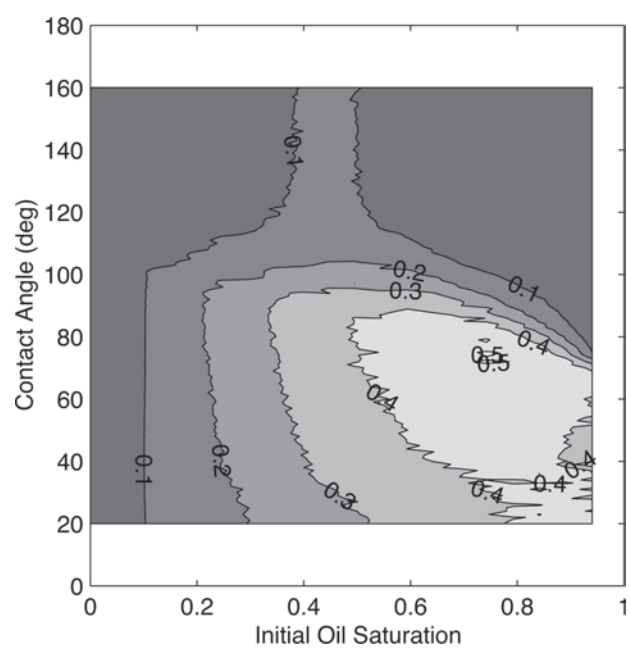

Fig. 3—Contour plot of the trapping surface. Trapped oil saturation depends on the initial oil saturation (S_{oi}) and rock wettability in terms of the intrinsic contact angle (θ).

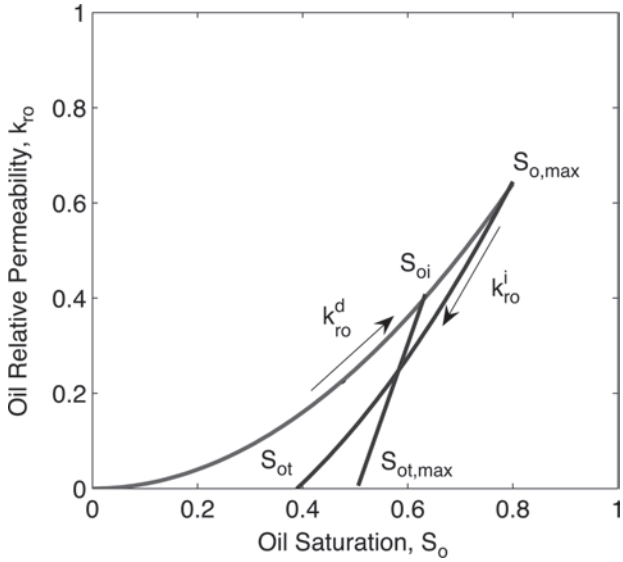

Fig. 4—Waterflood relative permeability curves that cross because of the nonmonotonic trapping relationship.

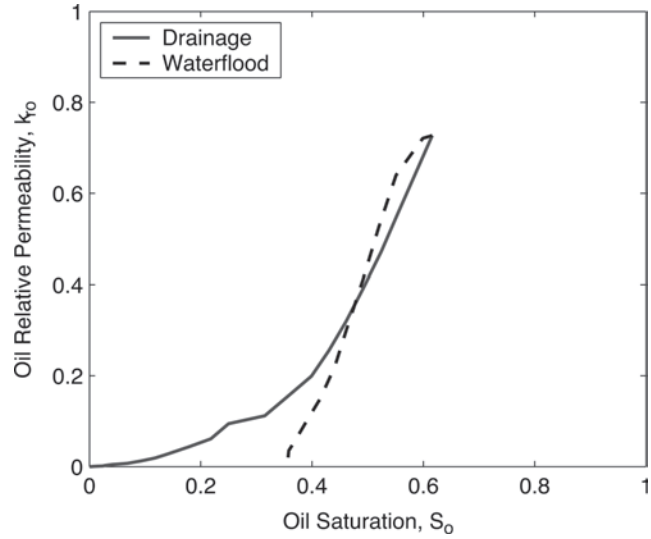

Fig. 5—Oil relative permeability curves for an water/oil system from Oak's (1990) experimental data in water-wet Berea sandstone.

not be generalized for the entire waterflood process. Because different competing trapping mechanisms may dominate at different capillary pressure levels, this affects the shape of the relative permeability curve.

In water-wet systems, we have already mentioned that trapping is primarily due to snap-off. After a certain point during waterflooding, the flowing oil phase becomes trapped because of the invading water phase. However, this mechanism does not operate right away. At the beginning of the waterflood process, the nonwetting-phase relative permeability is slightly higher than the drainage relative permeability. This is seen in the two-phase experiments performed by Oak (1990) in water-wet Berea sandstone (see **Fig. 5**).

During primary drainage, the oil preferentially fills large pores, leaving water residing in narrower throats and in the corners of the pore space. At the end of primary drainage, many oil-filled pores have only a single connecting throat that is also oil-filled. These dead-end pores may contain a large saturation but do not contribute to the connectivity of the oil. During waterflooding, pore-filling is favored in pores that have many surrounding water-filled throats, essentially these dead-end pores (Lenormand et al. 1983). Thus initially there is a cascade of pore-filling, where the oil saturation decreases with little decrease in oil relative permeability. This process competes with snap-off, which traps oil and in contrast leads to a large decrease in relative permeability. For water-wet media, the former process generally is more significant at high oil saturation, giving the typical hysteresis patterns seen in Fig. 5. The pore-network model is able to reproduce this behavior with a quantitative agreement with experiment (Valvatne and Blunt 2004); see **Fig. 6.**

In contrast, the trapping mechanisms that control the shape of the oil waterflood relative permeabilities in oil-wet media are very different from those of a water-wet rock. At the beginning of the waterflood, water percolates through the largest pores, leading to a significant reduction in the oil relative permeability. The oil, which remains connected through oil layers, drains down to very low saturations but at a low rate because of the small conductance of these layers. The shape of these relative permeability curves, as predicted by pore-network simulations, is shown in **Fig. 7.**

Development and Validation of a New Model of Relative Permeability Hysteresis

In the previous section, we used pore-network modeling to highlight the following features of wettability effects on the waterflood relative permeability:

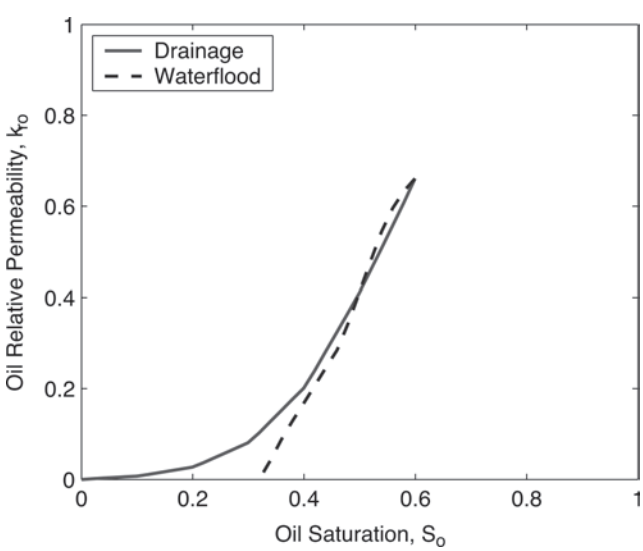

Fig. 6—Oil relative permeabilities generated from pore-network simulation in strongly water-wet media, $\theta_i \in [0°,20°]$.

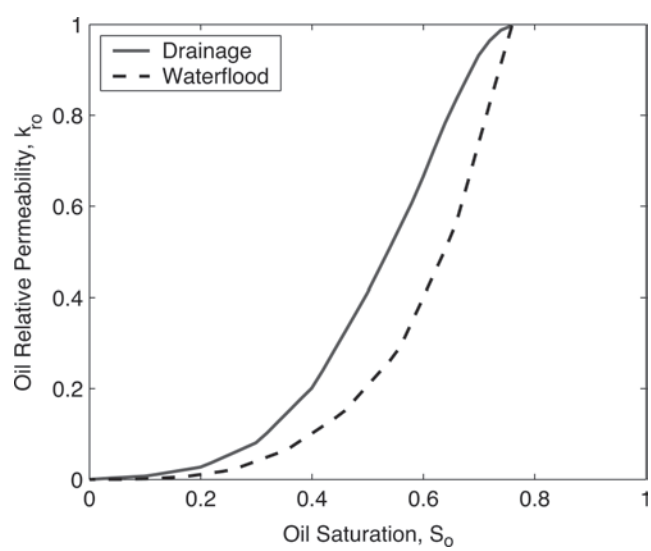

Fig. 7—Oil relative permeabilities generated from pore-network simulation in strongly oil-wet media, $\theta_i \in [160°,180°]$.

1. The IR curves are not monotonic for media that are not strongly water-wet (Fig. 2).

2. For intermediate-wet and oil-wet media, the scanning curves of oil relative permeability may cross (Fig. 4).

3. In strongly water-wet media, the trapped oil saturation is high, but the waterflood relative permeability may be higher than the drainage relative permeability at high oil saturations (Fig. 6).

4. In contrast, for strongly oil-wet media, the trapped oil saturation is low, but the waterflood relative permeability decreases sharply at high oil saturations (Fig. 7).

Clearly, this markedly different behavior in water-wet and oil-wet media needs to be incorporated in the empirical model. We start by describing a new trapping submodel, and we follow with the proposed waterflood relative permeability model.

The Trapping Model. We begin by reviewing some of the existing trapping models. These models were originally designed to account for gas trapping, but for consistency we will treat them for oil trapping. We then formulate a new model and assess its performance for the full spectrum of wettability conditions.

Land Trapping Model. The Land model (1968) is the most widely used empirical trapping model. Most relative permeability models that incorporate hysteresis (Jerauld 1997a; Killough 1976; Larsen and Skauge 1998; Lenhard and Parker 1987; Blunt 2000; Lenhard and Oostrom 1998) are based on it. It was developed to predict trapped gas saturation as a function of the initial gas saturation based on published experimental data from water-wet sandstone cores (Holmgren and Morse 1951; Kyte et al. 1956; Dardaganian 1957).

The trapped nonwetting phase saturation is computed as:

$$S_{ot}(S_{oi}) = \frac{S_{oi}}{1 + CS_{oi}}, \quad (1)$$

where S_{oi} is the initial oil saturation, or the saturation at the flow reversal, and C is the Land trapping coefficient.

The Land coefficient is computed from the bounding oil invasion and waterflood curves as follows:

$$C = \frac{1}{S_{ot,\max}} - \frac{1}{S_{o,\max}}, \quad (2)$$

where $S_{o,\max}$ is the maximum oil saturation, and $S_{ot,\max}$ is the maximum trapped oil saturation, associated with the bounding waterflood curve. All these quantities are illustrated in **Fig. 8.** The value of the Land trapping parameter is dependent on the type of rock and fluids (Spiteri and Juanes 2006).

Carlson Trapping Model. A simplified hysteresis model proposed by Carlson (1981) implicitly defines a trapping model. The Carlson model requires the bounding drainage and waterflood curves. The trapped oil saturation is determined by shifting the bounding waterflood curve to intersect the intermediate initial oil saturation at the flow reversal. The idea behind Carlson's interpretation is to use the model of the waterflood relative permeability scanning curves as being parallel to each other. This geometric extrapolation procedure is illustrated in **Fig. 9.**

The trapped nonwetting-phase saturation is computed as

$$S_{ot} = S_{ot,\max} - \Delta S_o, \quad (3)$$

where ΔS_o is the shift in the waterflood scanning curve with respect to the imbibition bounding curve (see Fig. 9).

This model is adequate if the intermediate scanning curves are almost parallel and there is little curvature in the waterflood curve. The model is problematic when the system is oil-wet. The large curvature of the bounding waterflood relative permeability curve at low saturations does not allow prediction of intermediate relative permeability curves, because any shifting will make the endpoint trapped gas saturation negative, a nonphysical value.

Jerauld Trapping Model. Jerauld's trapping model (1997a) is an extension of the Land trapping model that accounts for the "plateau" observed in the IR curves for mixed-wet rocks (1997b). The trapped nonwetting-phase saturation is given by:

$$S_{ot} = \frac{S_{oi}}{1 + CS_{oi}^{1+b/C}}. \quad (4)$$

In the original publication (Jerauld 1997a), the expression of the trapped saturation S_{ot} was given in terms of the residual saturation achieved when $S_{oi} = 1$, $S_{or} = 1/(C+1)$. Jerauld introduced a second tuning parameter b in addition to the Land coefficient. If this parameter is set to zero, Jerauld's model reduces to the Land trapping model. When this parameter is equal to one, the trapping curve has a zero slope at $S_{oi} = 1$. Although Jerauld argued that the IR curves should not have a negative slope, his model allows for such behavior if $b \geq 1$.

Although the fit of Jerauld's model to the pore-network data was good for water-wet and intermediate-wet conditions (for which the model was designed), it was not as satisfactory for strongly oil-wet media. One of the reasons is that Jerauld's model assumes that the IR curve has a unit slope near the origin. This behavior does not conform to pore-network predictions (see the curve corresponding to $\theta = 140°$ in Fig. 2).

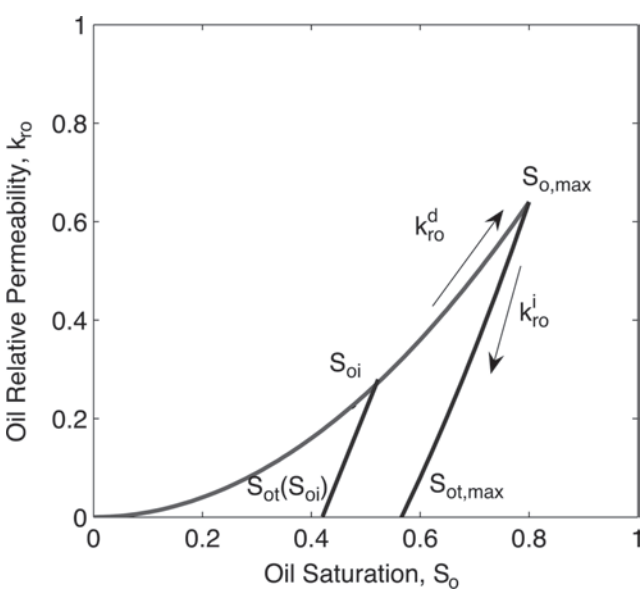

Fig. 8—Parameters required in the evaluation and application of the Land trapping model.

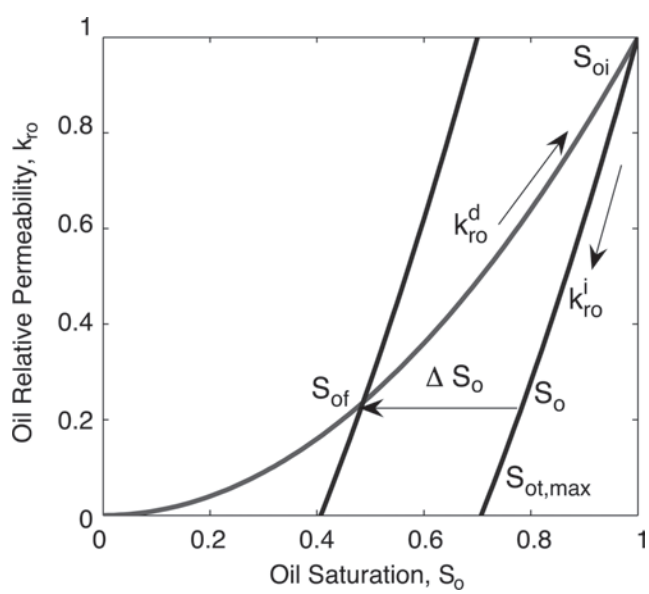

Fig. 9—Geometric extrapolation of the oil relative permeability and trapped saturation during waterflooding, as proposed by Carlson (1981).

A New Trapping Model. We notice that the shapes of the trapping curves (Fig. 2) may be fit to a parabola. We establish the following simple quadratic relationship between the trapped oil saturation S_{ot} and the initial oil saturation S_{oi}:

$$S_{ot} = \alpha S_{oi} - \beta S_{oi}^2. \quad (5)$$

The parameters α and β correspond to the initial slope and the curvature of this curve, respectively. These parameters were tuned to minimize the least squared error between the model prediction and the pore-network simulation data. The optimization is constrained by the following restrictions:

$$0 \le \alpha \le 1, \beta \ge 0. \quad (6)$$

For an initial slope greater than 1, the trapping model would predict more trapped oil than what was originally present, which is not physically possible. The "optimal" parameters α and β are shown in **Fig. 10** as functions of the intrinsic contact angle. The proposed trapping model has two parameters and, therefore, we expect a better fit to the pore network simulation results than the Land trapping model. The presence of an additional parameter is entirely justified, however, by the need to capture the non-monotonic behavior of the IR curves.

The performance of the optimization is illustrated in **Fig. 11.** Notice that for water-wet media, the model tends to slightly overestimate the trapped oil saturation when the initial oil saturation is high. This is because of the constraint in the optimization, and the inability of the model to achieve the desired curvature at the desired location. The important consideration is that the trapping model reproduces the observed trapping behavior for all wettability conditions, even if it may slightly overestimate the trapping of the bounding waterflood curve ($S_{oi} = S_{o,\max} = 1 - S_{wc}$). We should also mention that the pore-network simulator is likely to underestimate the trapping for the bounding curves because of an overly optimistic criterion for the stability of oil layers. If a new, free-energy based stability criterion is implemented (van Dijke et al. 2004), we expect a better agreement between the trapping model and the pore-network predictions.

When the parameters calculated from the optimization are employed, the resulting trapping surface is shown in **Fig. 12.** This surface should be compared with the one obtained from pore-network simulations (Fig. 3).

The Waterflood Relative Permeability Model. Most existing relative permeability hysteresis models (Jerauld 1997a; Killough 1976; Larsen and Skauge 1998; Lenhard and Parker 1987; Blunt 2000) either require a bounding waterflood curve or model this curve according to Land's (1968) waterflood relative permeability model. The development of his model is described next. The new relative permeability model we propose is an extension of Land's model to account for the different pore occupancies at different wettability conditions.

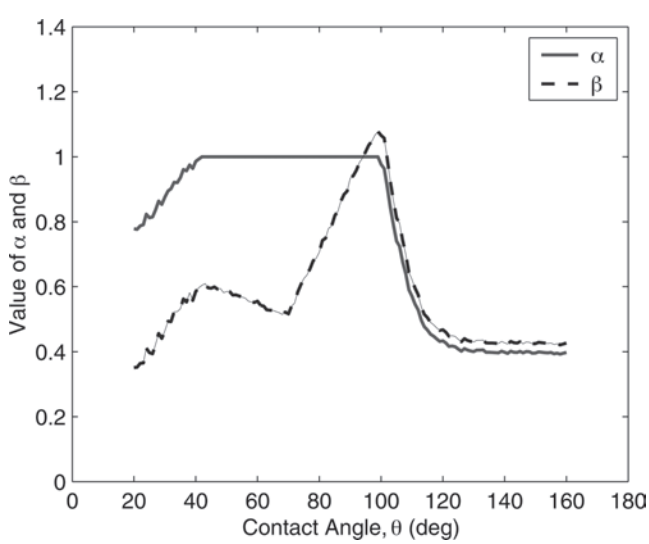

Fig. 10—Dependence of parameters α and β of the proposed quadratic trapping model on the intrinsic contact angle of initially oil-filled pores for a network model of a Berea sandstone.

Land Waterflood Model. As a prelude to the development of the new waterflood relative permeability model proposed in this work, we revisit the derivation of Land's relative permeability model. The basis of Land's formulation is to express the *waterflood* relative permeability k_{ro}^i at a given oil saturation (S_o) as being equal to the drainage permeability k_{ro}^d evaluated at a *flowing* oil saturation S_{of} (see **Fig. 13**):

$$k_{ro}^i(S_o) = k_{ro}^d(S_{of}). \quad (7)$$

At any bulk saturation S_o, the flowing oil saturation S_{of} and the trapped saturation ΔS_o are related by

$$\Delta S_o = S_o - S_{of}. \quad (8)$$

Land makes the assumption that the trapped saturation ΔS_o is the cumulative trapped saturation at a given point in the waterflood process and that this quantity increases as more of the flowing saturation becomes trapped. He assumes that the maximum amount of cumulative trapping, equal to the trapped saturation determined by his trapping model (Eq. 1) occurs when the flowing saturation becomes zero [$S_o = S_{ot}(S_{oi})$]. It is important to note that in Land's formulation, it is necessary to obtain the maximum trapped oil saturation $S_{ot,\max}$ from a coreflood experiment in order to extract the appropriate Land trapping coefficient C.

The intermediate trapped saturation ΔS_o is equal to the cumulative trapped saturation S_{ot} minus the amount of oil that is still flowing and will eventually be trapped:

$$\Delta S_o = S_{ot} - S_{ot}(S_{of}), \quad (9)$$

where

$$S_{ot} \equiv S_{ot}(S_{oi}) = \frac{S_{oi}}{1 + CS_{oi}}, \quad (10)$$

and

$$S_{ot}(S_{of}) = \frac{S_{of}}{1 + CS_{of}}. \quad (11)$$

Substituting Eqs. 9 through 11 in Eq. 8, one obtains

$$S_{of}^2 - (S_o - S_{ot})S_{of} - \frac{1}{C}(S_o - S_{ot}) = 0. \quad (12)$$

Solving this quadratic equation for S_{of} and taking the positive root:

$$S_{of} = \frac{1}{2}\left[(S_o - S_{ot}) + \sqrt{(S_o - S_{ot})^2 + \frac{4}{C}(S_o - S_{ot})}\right]. \quad (13)$$

Although Land's assumptions are generally valid for water-wet media, they do not hold for oil-wet media. In water-wet media, we noticed that the experimental and pore-network waterflood curves are sometimes above the drainage curves for high oil saturations (Figs. 5 and 6). Land's model will generally underestimate the relative permeabilities in this region under the assumption that the hydrocarbon phase will immediately be subjected to snap-off. In oil-wet media, the ultimate residual saturations are often very low because of oil layer drainage. Initially, there is a sharp decrease in the waterflood relative permeability (Fig. 7). However, at low oil saturations, oil layer drainage is the dominant mechanism, which leads to low oil residual saturations achieved at very low oil relative permeabilities.

In **Fig. 14,** we compare Land's waterflood relative permeability model to the pore-network simulation results. The thick red line is the drainage relative permeability curve, obtained from the pore network simulator. The blue circles correspond to the pore network imbibition curve and the thin blue line to the Land waterflood relative permeability model. The Land trapping model predicts the experimental data fairly well for water-wet media, but is unable to capture the convex shape of the waterflood curve characteristic of

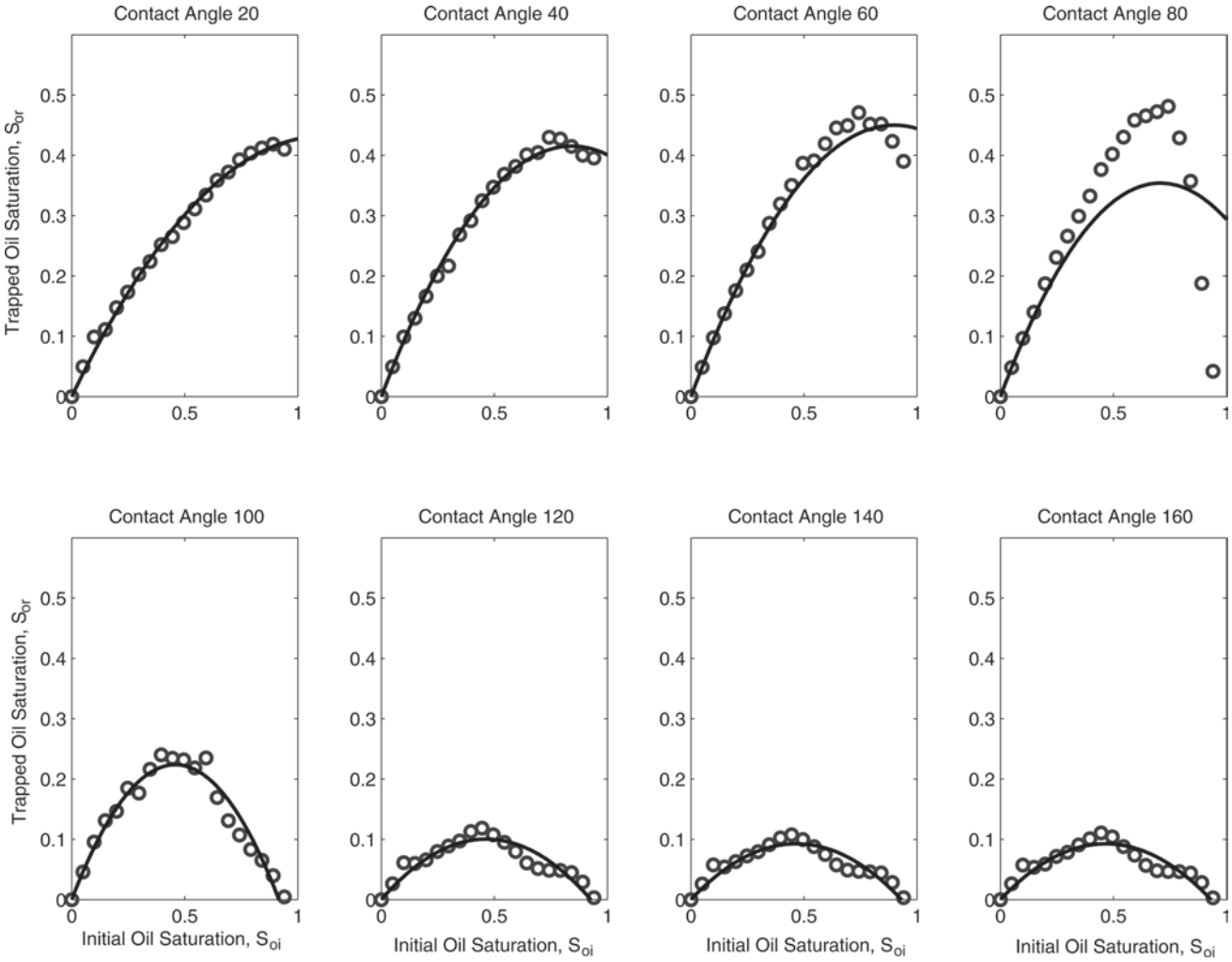

Fig. 11—Performance of the new trapping model: IR curves calibrated against pore-network simulation data.

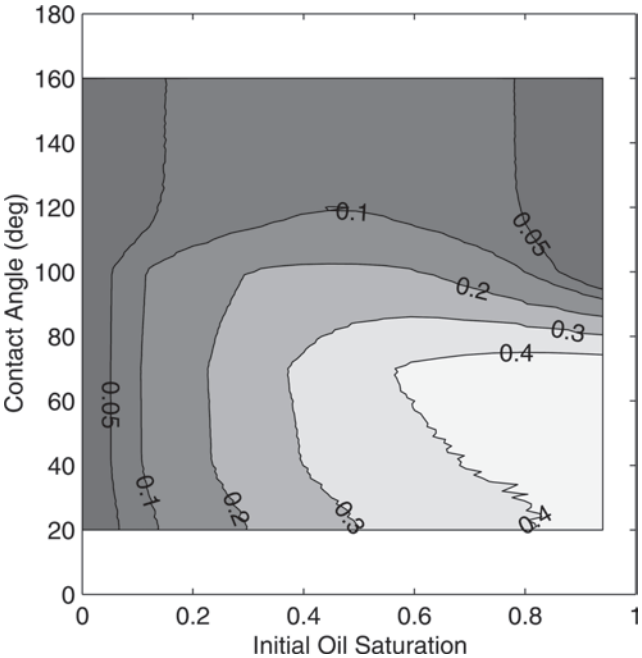

Fig. 12—Trapping surface determined with the new trapping model.

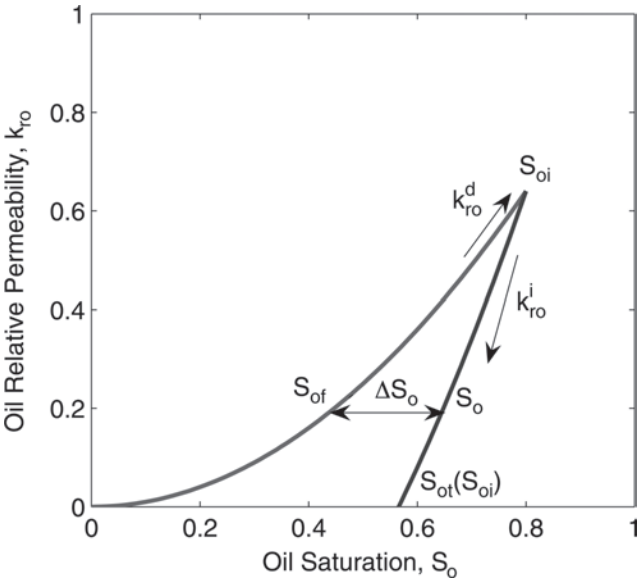

Fig. 13—Trapped and flowing saturations used to determine the waterflood relative permeability from the drainage relative permeability.

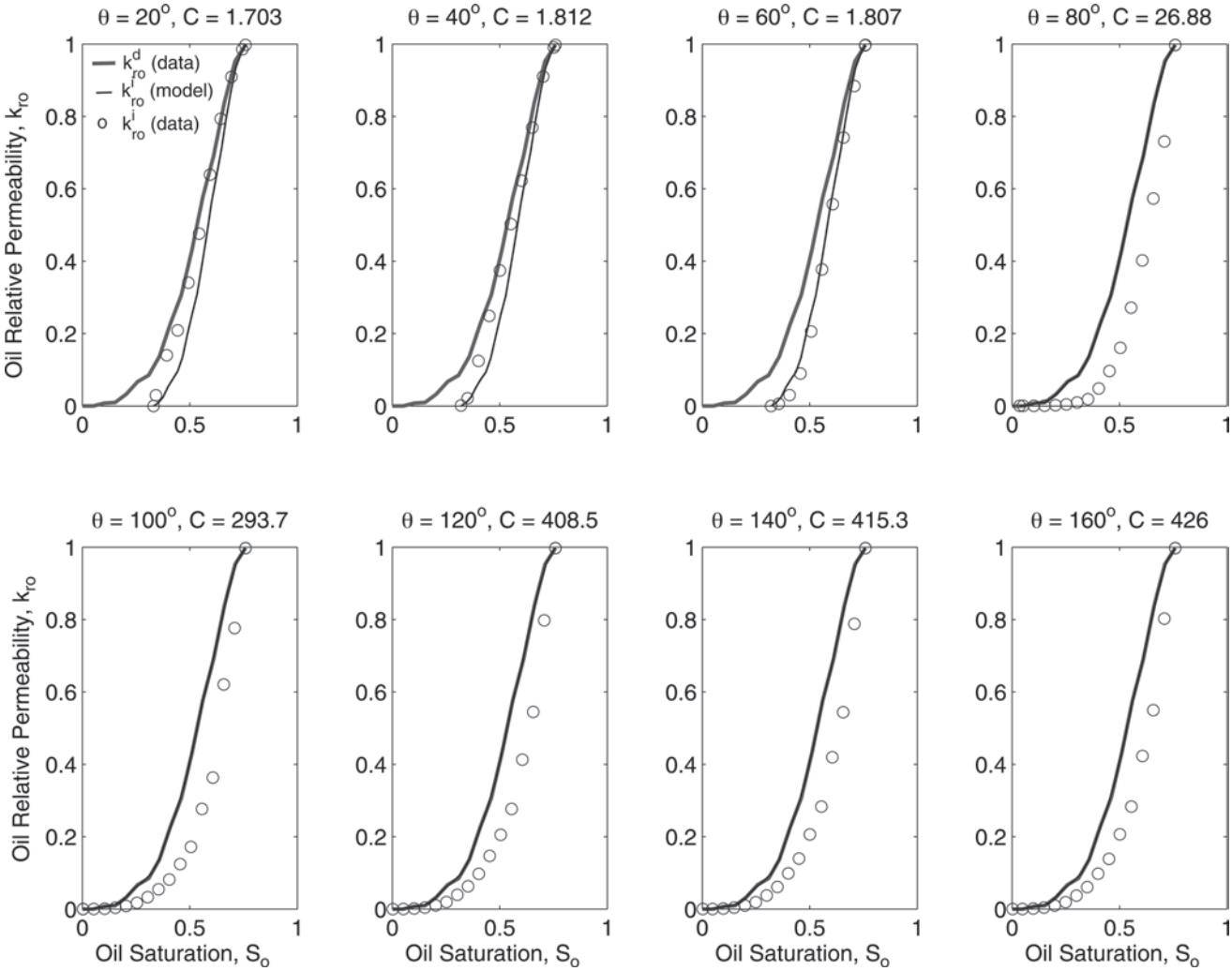

Fig. 14—Comparison of Land's trapping model for the bounding relative permeability curves with pore-network simulation data.

oil-wet conditions. Indeed, for intrinsic contact angles greater than 80°, Land's model predicts reversible relative permeability curves—waterflood relative permeability curves coincide with the primary drainage curves.

A New Waterflood Model. Land's waterflood model hinges on the assumption that the trapped saturation increases monotonically during waterflooding. This assumption does not allow reproduction of the convex shape of the observed relative permeability curves in intermediate-wet and oil-wet media. We modify Eq. 9 as follows:

$$\Delta S_o = S_{ot}(S_{oi}) - S_{ot}(S_{of}) - \gamma[S_o - S_{ot}(S_{oi})](S_o - S_{oi}). \quad (14)$$

The last term in this equation is designed to capture the convexity of the waterflood curves in oil-wet media. It satisfies the following essential requirements: (1) the flowing saturation S_{of} equals zero when the bulk saturation reaches the ultimate trapped saturation $S_{ot}(S_{oi})$; and (2) the flowing saturation is equal to the bulk saturation ($S_{of}=S_o$) at the beginning of the waterflood ($S_o=S_{oi}$) and no oil has yet been trapped. The parameter γ is an additional parameter of the formulation, which should depend on rock type and wettability characteristics.

Substituting Eq. 14 into Eq. 8, we obtain

$$S_{of} = S_o - S_{ot}(S_{oi}) + S_{ot}(S_{of}) + \gamma[S_o - S_{ot}(S_{oi})](S_o - S_{oi}), \quad (15)$$

where the trapped saturation is given by the new trapping model:

$$S_{ot}(S_{oi}) = \alpha S_{oi} - \beta S_{oi}^2. \quad (16)$$

We substitute Eq. 16 in Eq. 15 and solve for S_{of}, to obtain a new model for the flowing oil saturation:

$$S_{of} = \frac{1}{2\beta}\left[(a-1) + \sqrt{(\alpha-1)^2 + 4\beta[S_o - S_{ot} + \gamma(S_o - S_{ot})(S_o - S_{oi})]}\right]. \quad (17)$$

This expression of the flowing saturation is then used in Eq. 7 to evaluate the waterflood relative permeability.

The tuning parameter can be obtained from fitting the model to experimental bounding waterflood curves. In this investigation, we used bounding waterflood curves obtained from pore-network simulation. The dependence of the parameter on the intrinsic contact angle is shown in **Fig. 15.** The trends in this relationship are the ones expected. For water-wet media, the parameter is negative, indicating that the Land trapping model overestimates the trapped saturation and subsequently underestimates the relative permeability. For oil-wet media, this parameter takes positive values, which allows for the model waterflood curve to be below the one predicted by the Land model.

The performance of the combined trapping and waterflood models is shown in **Fig. 16.** Unlike Land's trapping model, the new model provides a suitable fit to the bounding waterflood curves determined by pore-network simulations for all contact angles. The dark circle represents the trapped saturation determined from the new trapping model. The trapped saturations predicted by the model do not always match the experimental endpoints. This is why the model relative permeabilities do not fully agree with the pore-network results, especially for saturations close to the ultimate residual saturation.

In **Fig. 17,** we compare the new waterflood model with pore-network simulated data for a set of intermediate scan-

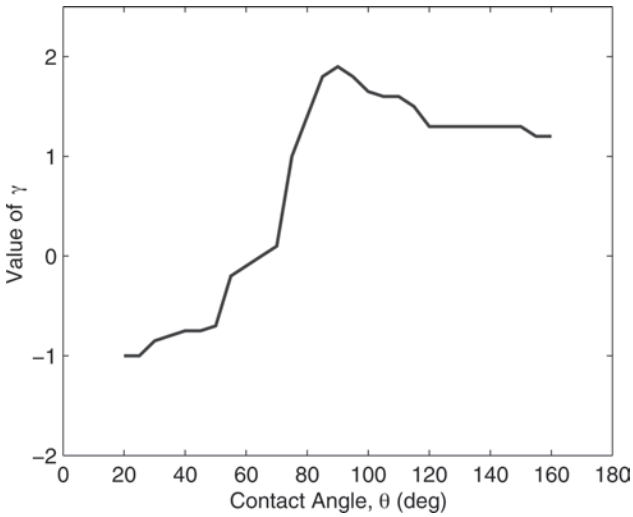

Fig. 15—Dependence of parameter of the proposed waterflood relative permeability model on the intrinsic contact angle of initially oil-filled pores for a network model of a Berea sandstone.

ning curves. Model predictions were obtained using the same parameters determined from the trapping curves and the bounding waterflood curves.

Wettability Correlations. In this paper, we have consistently used the intrinsic contact angle θ_i as a measure of wettability. This parameter is almost impossible to determine with any certainty in the laboratory because most rocks are characterized by a large range of contact angles. Moreover, we have used a particular model (Morrow 1975) that links the intrinsic contact angle with the receding and advancing contact angles.

Ideally, one would correlate the trapping parameters α and β and the waterflood parameter with a measure of the overall wettability characteristics of the rock that can be determined in the lab. In fact, previous investigations (Øren and Bakke 2003; Valvatne and Blunt 2004) have shown that pore-network models are able to perform quantitative predictions of laboratory wettability measurements.

Common measures of wettability are the Amott wettability indices I_w and I_o (1959). A strongly water-wet medium is associated with $I_w = 1$ and $I_o = 0$, while values of $I_w = 0$ and $I_o = 1$ correspond to a strongly oil-wet medium. The Amott-Harvey index I_{wo} is probably the most popular measure of wettability and is defined as

$$I_{wo} = I_w - I_o, \quad \ldots\ldots\ldots\ldots\ldots\ldots\ldots\ldots\ldots\ldots\ldots\ldots (18)$$

which ranges between –1 and 1.

These indices can be determined from two capillary pressure curves corresponding to waterflood and subsequent oilflood, and can be computed directly from pore-network simulations (Øren and Bakke 2003; Valvatne and Blunt 2004). The variability of the Amott oil and water indices and the Amott-Harvey wettability index with respect to the intrinsic contact angle is given in **Figs. 18 and 19,** respectively. Although this was not pursued here, one could express the dependence of the trapping and waterflood relative permeability parameters with respect to the Amott-Harvey wettability index directly, rather than the intrinsic contact angle.

Conclusions

We have presented a new model of trapping and waterflood relative permeability. Development of the model is motivated by the inability of existing models to capture the trends observed for intermediate-wet and oil-wet media. Because of scarcity of reliable experimental data, we have used pore-network simulation as a means to predict the trends in trapping and relative permeability hysteresis. The new model is able to capture two key features of the observed behavior: (1) non-monotonicity of the IR curves, which implies that waterflood relative permeabilities cross; and (2) convexity of the waterflood relative permeability curves for oil-wet media caused by layer flow of oil.

The developments presented here are restricted to two-phase flow. We plan to extend the formulation for trapping and waterflood relative permeability for three phase flow and, in particular, for waterflood after gas injection (Spiteri and Juanes 2006).

Nomenclature

b = exponent parameter in Jerauld's trapping model
C = Land trapping coefficient
I_o = Amott oil wettability index
I_w = Amott water wettability index
I_{wo} = Amott-Harvey wettability index
k_{rw} = water relative permeability
k_{ro}^d = drainage oil relative permeability
k_{ro}^i = waterflood oil relative permeability
S_o = oil saturation
$S_{o,\max}$ = maximum oil saturation
S_{of} = flowing oil saturation
S_{oi} = initial oil saturation
S_{ot} = ultimate trapped oil saturation
S_w = water saturation
ΔS_o = intermediate trapped oil saturation
α = initial slope of IR curve in new trapping model
β = curvature of the IR curve in new trapping model
γ = layer flow parameter in new waterflood model
θ, θ_i = intrinsic contact angle
θ_a = advancing contact angle
θ_r = receding contact angle

Acknowledgments

Spiteri, Juanes, and Orr gratefully acknowledge financial support from the industrial affiliates of the Stanford University Petroleum Research Institute for Gas Injection (SUPRI-C). Blunt would like to thank the sponsors of the Imperial College Consortium on Pore-Scale Modeling and NERC for funding.

References

Al-Futaisi, A. and Patzek, T.W. 2003. Impact of wettability on two-phase flow characteristics of sedimentary rock: A quasi-static description. *Water Resources Research* **39** (2): 1042. DOI:10.1029/2002WR001366.

Al-Futaisi, A. and Patzek, T.W. 2004. Secondary imbibition in NAPL-invaded mixed-wet sediments. *J. Contaminant Hydrol.* **74** (1–4): 61–81. DOI:10.1016/j.jconhyd.2004.02.005.

Amott, E. 1959. Observations Relating to the Wettability of Porous Rock. *Trans.,* AIME, **216:** 156–162.

Bakke, S. and Øren, P-E. 1997. 3-D Pore-Scale Modelling of Sandstones and Flow Simulations in the Pore Networks. *SPEJ* **2** (2): 136–149. SPE-35479-PA. DOI: 10.2118/35479-PA.

Blunt, M.J. 2000. An Empirical Model for Three-Phase Relative Permeability. *SPEJ* **5** (4): 435–445. SPE-67950-PA. DOI: 10.2118/67950-PA.

Blunt, M.J. 2001. Flow in porous media—Pore network models and multiphase flow. *Curr. Opin. Colloid Interface Sci.* **6** (3): 197–207. DOI:10.1016/S1359-0294(01)00084-X.

Blunt, M.J. and King, P. 1991. Relative permeabilities from two- and three-dimensional pore-scale network modeling. *Transport in Porous Media* **6** (4): 407–433. DOI:10.1007/BF00136349.

Blunt, M.J., Jackson, M.D., Piri, M., and Valvatne P.H. 2003. Detailed physics, predictive capabilities and macroscopic consequences for pore-network models of multiphase flow. *Advances in Water Resources* **25** (8–12): 1069–1089. DOI:10.1016/S0309-1708(02)00049-0.

Bryant, S. and Blunt, M.J. 1992. Prediction of relative permeability in simple porous media. *Phys. Rev. A* **46** (4): 2004–2011. DOI:10.1103/PhysRevA.46.2004.

Carlson, F.M. 1981. Simulation of Relative Permeability Hysteresis to the Nonwetting Phase. Paper SPE 10157 presented at the SPE Annual

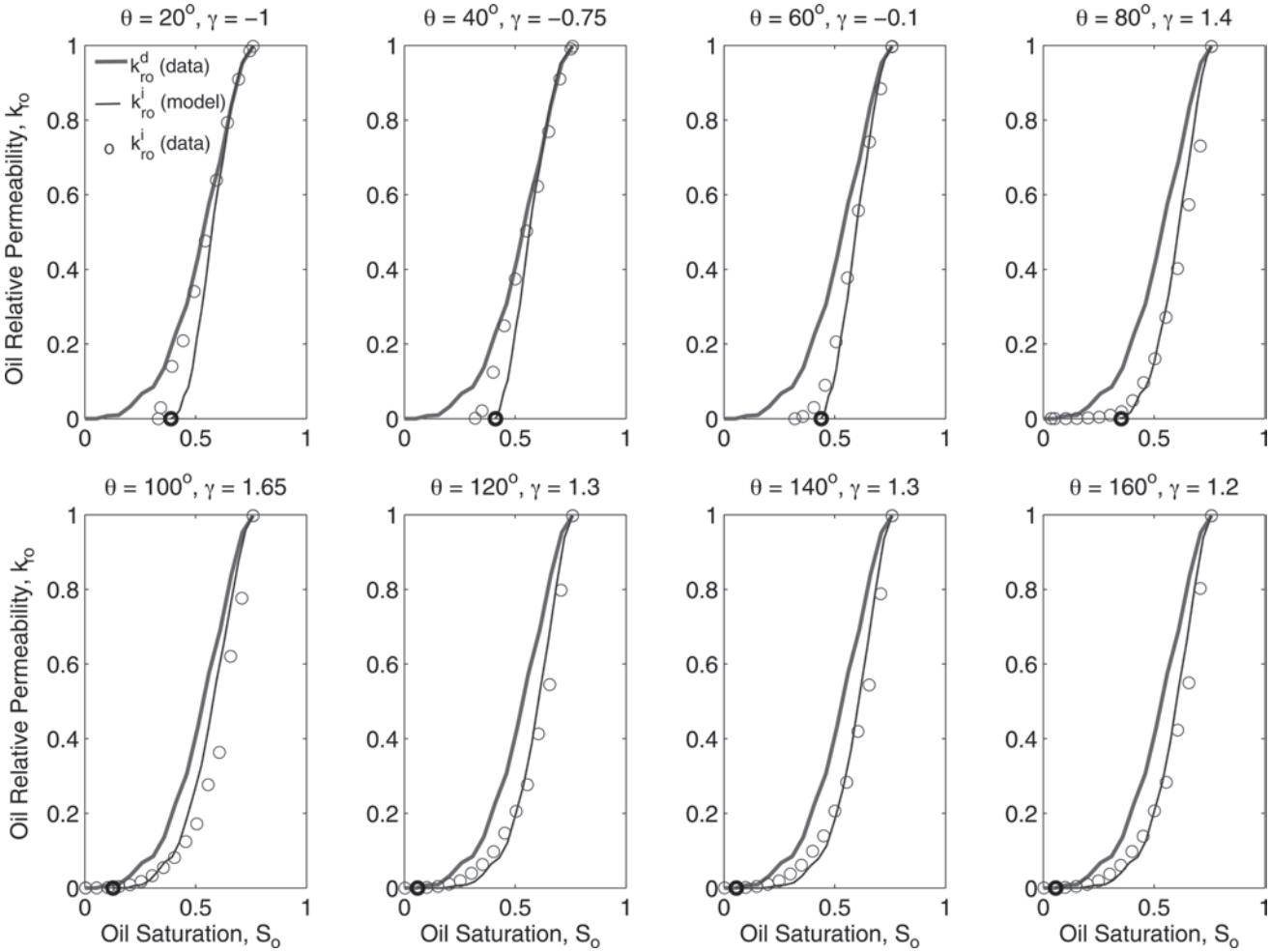

Fig. 16—Comparison of the new waterflood model with pore-network simulation data for the bounding relative permeability curves (initial saturation S_{oi}=0.76).

Technical Conference and Exhibition, San Antonio, Texas, USA, 4–7 October. DOI: 10.2118/10157-MS.

Chatzis, I., Morrow, N.R., and Lim, H.T. 1983. Magnitude and Detailed Structure of Residual Oil Saturation. *SPEJ* **23** (2): 311–330. SPE-10681-PA. DOI: 10.2118/10681-PA.

Dardaganian, S.G. 1957. The displacement of gas by oil in the presence of connate water. MS thesis, Texas A&M University, College Station, Texas.

Dixit, A.B., McDougall, S.R., Sorbie, K.S., and Buckley, J.S. 1999. Pore-Scale Modeling of Wettability Effects and Their Influence on Oil Recovery. *SPEREE* **2** (1): 25–36. SPE-54454-PA. DOI: 10.2118/54454-PA.

Donaldson, E.C., Thomas, R.D., and Lorenz, P.B. 1969. Wettability Determination and its Effect on Recovery Efficiency. *SPEJ* **9** (1): 13–20; *Trans.,* AIME, **246**. SPE-2338-PA. DOI: 10.2118/2338-PA.

Egermann, P., Vizika, O., Dallet, L., Requin, C., and Sonier, F. Hysteresis in Three-Phase Flow: Experiments, Modeling and Reservoir Simulations. Paper SPE 65127 presented at the SPE European Petroleum Conference, Paris, 24–25 October. DOI: 10.2118/65127-MS.

Element, D.J., Masters, J.H.K., Sargent, N.C., Jayasekera, A.J., and Goodyear, S.G. 2003. Assesment of Three-Phase Relative Permeability Models Using Laboratory Hysteresis Data. Paper SPE 84903 presented at the SPE International Improved Oil Recovery Conference in Asia Pacific, Kuala Lumpur, 20–21 October. DOI: 10.2118/84903-MS.

Fatt, I. 1956. The Network Model of Porous Media. *Trans.,* AIME, **207:** 144–159.

Geffen, T.M., Owens, W.W., Parrish, D.R., and Morse, R.A. 1951. Experimental Investigation of Factors Affecting Laboratory Relative Permeability Measurements. *Trans.,* AIME, **192:** 99–110.

Holmgren, C.R. and Morse R.A. 1951. Effect of Free Gas Saturation on Oil Recovery by Water Flooding. *Trans.,* AIME, **192:** 135–140.

Holt, R.M., Fjaer, E., Torsaeter, O., and Bakke, S. 1996. Petrophysical laboratory measurements for basin and reservoir evaluation. *Marine and Petroleum Geology* **13** (4): 383–391. DOI:10.1016/0264-8172(95)00091-7.

Ioannidis, M.A. and Chatzis, I. 2000. On the geometry and topology of 3D stochastic porous media. *J. Colloid Interface Sci.* **229** (2): 323–334. DOI:10.1006/jcis.2000.7055.

Jackson, M.D., Valvatne, P.H., and Blunt, M.J. 2003. Prediction of wettability variation and its impact on flow using pore- to reservoir-scale simulations. *J. Pet. Sci. Eng.* **39** (3–4): 231–246. DOI:10.1016/S0920-4105(03)00065-2.

Jadhunandan, P.P. and Morrow, N.R. 1995. Effect of Wettability on Waterflood Recovery for Crude-Oil/Brine/Rock Systems. *SPERE* **10** (1): 40–46. SPE-22597-PA. DOI: 10.2118/22597-PA.

Jerauld, G.R. 1997a. General Three-Phase Relative Permeability Model for Prudhoe Bay. *SPERE* **12** (4): 255–263. SPE-36178-PA. DOI: 10.2118/36178-PA.

Jerauld, G.R. 1997b. Prudhoe Bay Gas/Oil Relative Permeability. *SPERE* **12** (1): 66–73. SPE-35718-PA. DOI: 10.2118/35718-PA.

Kennedy, H.T., Burja, E.O., and Boykin, R.S. 1955. An investigation of the effects of wettability on the recovery of oil by water flooding. *J. Physical Chem.* **59** (9): 867–869. DOI:10.1021/j150531a015.

Killough, J.E. 1976. Reservoir Simulation With History-Dependent Saturation Functions. *SPEJ* **16** (1): 37–48; *Trans.,* AIME, **261**. SPE-5106-PA. DOI: 10.2118/5106-PA.

Kossack, C.A. 2000. Comparison of Reservoir Simulation Hysteresis Options. Paper SPE 63147 presented at the SPE Annual Technical Conference and Exhibition, Dallas, 1–4 October. DOI: 10.2118/63147-MS.

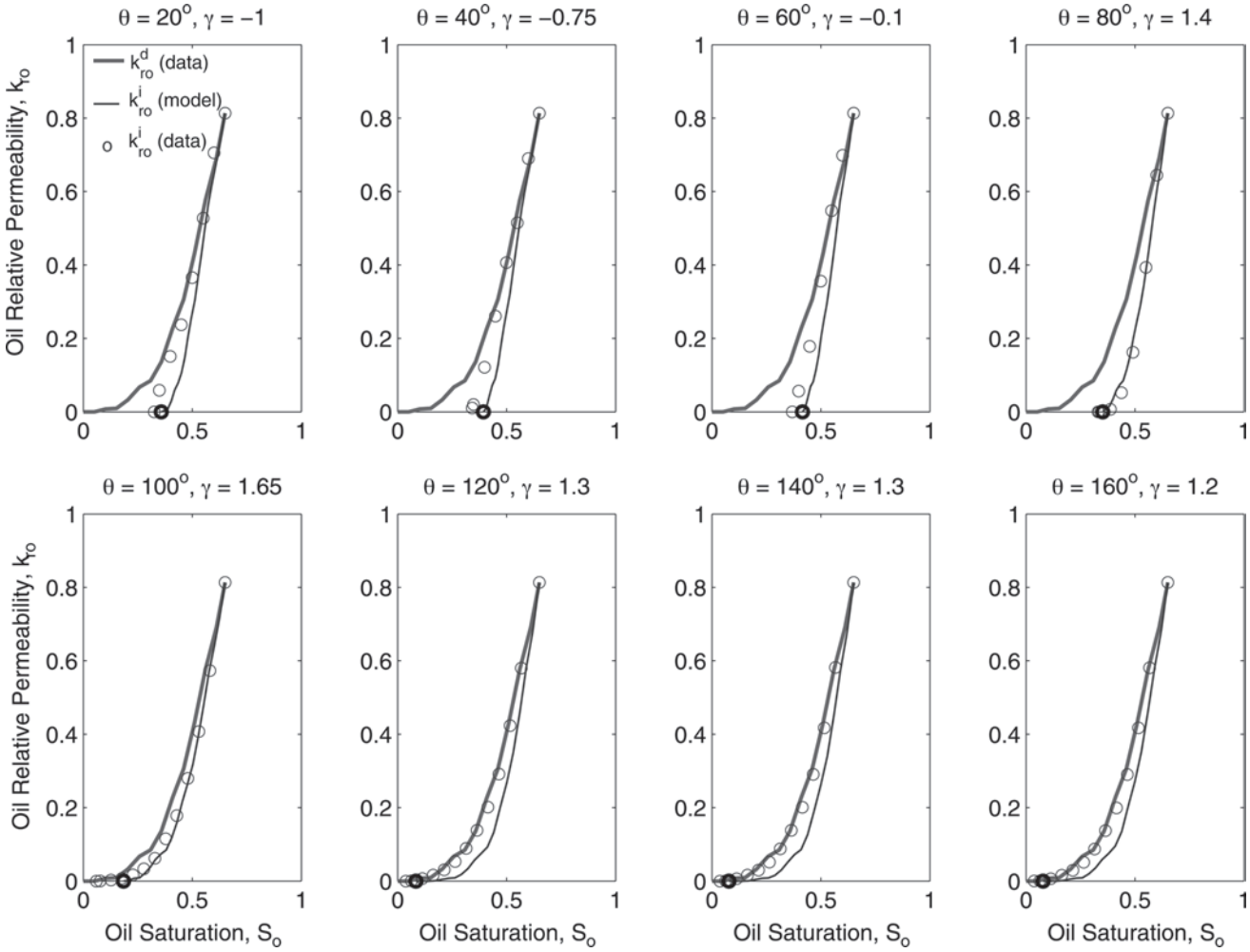

Fig. 17—Comparison of the new waterflood model with pore-network simulation data for the scanning relative permeability curves (initial saturation S_{oi}=0.65).

Kovscek, A.R., Wong, H., and Radke, C.J. 1993. A pore-level scenario for the development of mixed wettability in oil reservoirs. *AIChE Journal* **39** (6): 1072–1085. DOI:10.1002/aic.690390616.

Kyte, J.R., Stanclift, R.J. Jr., Stephan, S.C. Jr., and Rapoport, L.A. 1956. Mechanism of Water Flooding in the Presence of Free Gas. *Trans.,* AIME, **207:** 215–221.

Land, C.S. 1968. Calculation of Imbibition Relative Permeability for Two- and Three-Phase Flow From Rock Properties. *SPEJ* **8** (2): 149–156; *Trans.,* AIME, **243**. SPE-1942-PA. DOI: 10.2118/1942-PA.

Land, C.S. 1971. Comparison of Calculated With Experimental Imbibition Relative Permeability. *SPEJ* **11** (4): 419–425; *Trans.,* AIME, **251**. SPE-3360-PA. DOI: 10.2118/3360-PA.

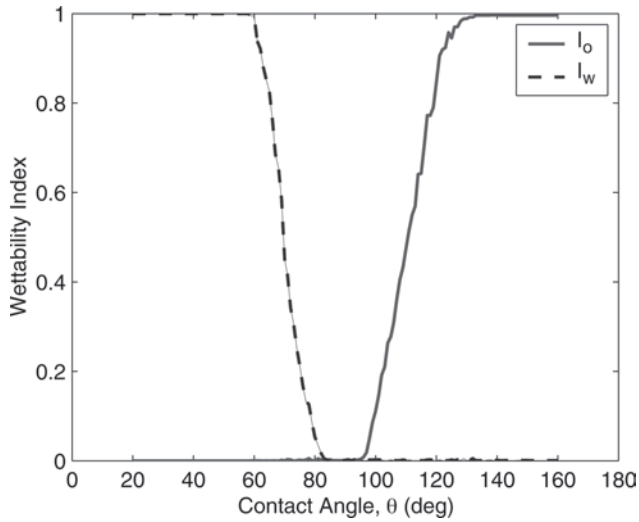

Fig. 18—Amott oil and water wettability indices for all intrinsic contact angles.

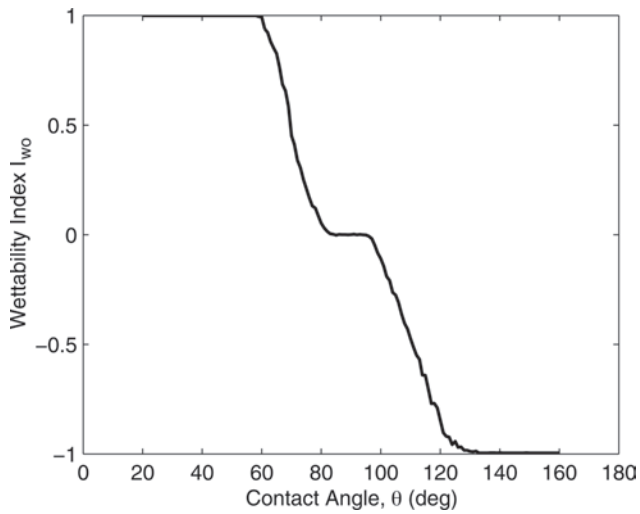

Fig. 19—Amott-Harvey wettability index for all intrinsic contact angles.

Larsen, J.A. and Skauge, A. 1998. Methodology for numerical simulation with cycle-dependent relative permeabilities. *SPEJ* **3** (2): 163–173. SPE-38456-PA. DOI: 10.2118/38456-PA.

Lenhard, R.J. and Oostrom, M. 1998. A parametric model for predicting relative permeability-saturation-capillary pressure relationships of oil-water systems in porous media with mixed wettability. *Transport in Porous Media* **31** (1): 109–131. DOI:10.1023/A:1006503406056.

Lenhard, R.J. and Parker, J.C. 1987. A model for hysteretic constitutive relations governing multiphase flow 2. Permeability-saturation relations. *Water Resources Research* **23** (12): 2197–2206. DOI:10.1029/WR023i012p02197.

Lenormand, R., Zarcone, C., and Sarr, A. 1983. Mechanisms of the displacement of one fluid by another in a network of capillary ducts. *J. Fluid Mech.* **135:** 337–353. DOI:10.1017/S0022112083003110.

Moore, T.F. and Slobod, R.L. 1956. The effect of viscosity and capillarity on the displacement of oil by water. *Prod. Monthly* **20** (10): 20–30.

Morrow, N.R. 1975. The effects of surface roughness on contact angle with special reference to petroleum recovery. *J. Can. Pet. Tech.* **14** (October–December): 42–54.

Moulu, J-C., Vizika, O., Egermann, P., and Kalaydjian, F. 1999. A New Three-Phase Relative Permeability Model for Various Wettability Conditions. Paper SPE 56477 presented at the SPE Annual Technical Conference and Exhibition, Houston, 3–6 October. DOI: 10.2118/56477-MS.

Oak, M.J. 1990. Three-Phase Relative Permeability of Water-Wet Berea. Paper SPE 20183 presented at the SPE/DOE Enhanced Oil Recovery Symposium, Tulsa, 22–25 April. DOI: 10.2118/20183-MS.

Oak, M.J. 1991. Three-Phase Relative Permeability of Intermediate-Wet Berea Sandstone. Paper SPE 22599 presented at the SPE Annual Technical Conference and Exhibition, Dallas, 6–9 October. DOI: 10.2118/22599-MS.

Øren, P-E. and Bakke, S. 2002. Process based reconstruction of sandstones and prediction of transport properties. *Transport in Porous Media* **46** (2–3): 311–343. DOI:10.1023/A:1015031122338.

Øren, P-E. and Bakke, S. 2003. Reconstruction of Berea sandstone and pore-scale modelling of wettability effects. *J. Pet. Sci. Eng.* **39** (3–4): 177–199. DOI: 10.1016/S0920-4105(03)00062-7.

Øren, P-E., Bakke, S., and Arntzen, O.J. 1998. Extending Predictive Capabilities to Network Models. *SPEJ* **3** (4): 324–336. SPE-52052-PA. DOI: 10.2118/52052-PA.

Owens, W.W. and Archer, D.L. 1971. The Effect of Rock Wettability on Oil-Water Relative Permeability Relationships. *JPT* **23** (7): 873–878. SPE-3034-PA. DOI: 10.2118/3034-PA.

Patzek T.W. 2001. Verification of a Complete Pore Network Simulator of Drainage and Imbibition. *SPEJ* **6** (2): 144–156. SPE-71310-PA. DOI: 10.2118/71310-PA.

Spanne, P., Thovert, J.F., Jacquin, C.J., Lindquist, W.B., Jones, K.W., and Adler, P.M. 1994. Synchrotron computed microtomography of porous media: topology and transports. *Phys. Rev. Lett.* **73** (14): 2001–2004. DOI: 10.1103/PhysRevLett.73.2001.

Spiteri, E.J. and Juanes, R. 2006. Impact of relative permeability hysteresis on the numerical simulation of WAG injection. *J. Pet. Sci. Eng.* **50** (2): 115–139. DOI:10.1016/j.petrol.2005.09.004.

Valvatne, P.H. and Blunt, M.J. 2004. Predictive pore-scale modeling of two-phase flow in mixed wet media. *Water Resources Research* **40:** W07406. DOI:10.1029/2003WR002627.

van Dijke, M.I.J., Lago, M., Sorbie, K.S., and Araujo M. 2004. Free energy balance for three fluid phases in a capillary of arbitrarily shaped cross-section: Capillary entry pressures and layers of the intermediate-wetting phase. *J. Colloid Interface Sci.* **277** (1): 184–201. DOI:10.1016/j.jcis.2004.05.021.

Elizabeth Spiteri is a Petroleum Reservoir Engineer at Chevron Energy Technology Company. e-mail: espiteri@chevron.com. Her current work focuses on performing simulation studies for reservoir appraisal and development, currently in West Africa basins of Nigeria and Angola. Her research interests include CO_2 sequestration, upscaling and multiscale methods, and 4D seismic inversion problems. She holds a BS degree in civil and environmental engineering from the University of Michigan, and an MS degree in petroleum engineering from Stanford University. She serves as a technical editor for *SPE Reservoir Evaluation & Engineering Journal.* **Ruben Juanes** is the ARCO assistant professor in Energy Studies, Department of Civil and Environmental Engineering, Massachusetts Institute of Technology. e-mail: juanes@mit.edu. Before joining the MIT faculty in 2006, he was acting assistant professor in petroleum engineering at Stanford University, where he was Elizabeth Spiteri's research advisor. His interest is in the theory and simulation of multiphase flow through porous media, with application to enhanced oil recovery by gas injection, geological CO_2 sequestration, and methane hydrates in nature. He holds MS and PhD degrees in civil and environmental engineering from the University of California at Berkeley. **Martin J. Blunt** is Professor of Petroleum Engineering and head of the Department of Earth Science and Engineering at Imperial College, London. e-mail: m.blunt@imperial.ac.uk. He previously was an associate professor at Stanford University and worked at the BP Research Centre. He holds MA and PhD degrees in physics from Cambridge University. Blunt, winner of the 1996 Cedric K. Ferguson Medal, served as Associate Executive Editor of *SPEJ* from 1996–98 and was on the Editorial Board from 1996-2005. He is a member of the London Board of the SPE. Blunt was a 2001 Distinguished Lecturer. **Franklin M. Orr, Jr.** is the Keleen and Carlton Beal Professor in Petroleum Engineering, Department of Energy Resources Engineering, and Director of the Global Climate and Energy Project at Stanford University. e-mail: fmorr@stanford.edu. He served as Dean, School of Earth Sciences, Stanford University from 1994-2002. Previously he held the positions of head of the miscible flooding section at the New Mexico Petroleum Recovery Research Center; Adjunct Associate Professor of Petroleum Engineering at New Mexico Institute of Mining and Technology; and research engineer at the Shell Development Company, Bellaire Research Center. He holds a BS degree from Stanford University and a PhD degree from the University of Minnesota, both in chemical engineering.